

**Development and evaluation of a new colorimetric DGT technique
for the 2D visualisation of labile phosphate in soils**

Author

Macias Arias, David, Teasdale, Peter R, Doolette, Casey L, Lombi, Enzo, Farquhar, Sarah,
Huang, Jianyin

Published

2021

Journal Title

Chemosphere

Version

Accepted Manuscript (AM)

DOI

[10.1016/j.chemosphere.2020.128704](https://doi.org/10.1016/j.chemosphere.2020.128704)

Rights statement

© 2020 Elsevier Ltd. This manuscript version is made available under the CC-BY-NC-ND
4.0 license <https://creativecommons.org/licenses/by-nc-nd/4.0/>

Downloaded from

<http://hdl.handle.net/10072/423393>

Griffith Research Online

<https://research-repository.griffith.edu.au>

1 Development and Evaluation of a New
2 Colorimetric DGT Technique for the 2D
3 Visualisation of Labile Phosphate in Soils

4 *David Macias Arias*^{1,2}, *Peter R. Teasdale*^{1,3}, *Casey L. Doolette*³, *Enzo Lombi*³, *Sarah*
5 *Farquhar*¹ and *Jianyin Huang*^{1,3*}

6
7 ¹ University of South Australia, UniSA STEM, Scarce Resources and Circular Economy
8 (ScaRCE), SA, 5095, Australia

9 ² School of Civil Engineering (ETSICCP), Universitat Politècnica de València, Camino
10 de Vera s/n, E-46022 Valencia, Spain

11 ³ University of South Australia, Future Industries Institute, SA, 5095, Australia

12
13 *Corresponding Author: leslie.huang@unisa.edu.au

16 **Abstract**

17 A new colorimetric technique for the measurement of labile phosphate in soils using the diffusive
18 gradients in thin films (DGT) technique was developed in this study. This technique can determine
19 the mass of phosphate accumulated on the precipitated Zr-oxide based binding gel by forming the
20 blue colour following the standard molybdate-ascorbic acid method. The optimal reaction
21 temperature and coloration time were 20°C (room temperature) and 26 minutes. After determining
22 a well-fitted calibration equation, the technique was able to measure phosphate concentration up
23 to 2.5 mg/L for 24 h deployment with a detection limit of 10.1 µg/L. Two-dimensional quantitative
24 visualisation of phosphate diffusion in three phosphorus (P) fertilised soils were obtained using
25 the colorimetric technique. The results from the colorimetric DGT technique were compared to
26 the elution DGT technique and Colwell P extraction. The DGT techniques (colorimetric and
27 elution) and Colwell P measurements demonstrated similar patterns of phosphate diffusion in soil.
28 Both DGT techniques showed similar phosphate concentration along the concentric rings around
29 the fertiliser application. A new, convenient, and fast DGT colorimetric technique was developed,
30 and successfully used to measure the distribution of potentially available phosphate in soils. The
31 new technique is less laborious than current techniques as it does not require any pre-treatment of
32 the binding gel layers or heating during scanning, thus providing faster results. Therefore, the
33 technique may be more suitable for in-field applications and can be used to investigate the *in situ*
34 diffusion of potentially available phosphate from fertilisers, and relate this to the plant uptake of
35 P.

36

37 Keywords: diffusive gradients in thin films; colorimetric staining technique; elution technique;
38 fertilised soils; two-dimensional measurement

39 **1. Introduction**

40 Phosphorus (P) is often a limiting nutrient for crop production. In Australia, most soils are deficient
41 in P, and farming therefore relies on the use of P fertilisers (Lombi et al., 2005; White et al., 2010).
42 Granular fertilisers, such as superphosphates and monoammonium phosphates (MAP), are
43 commonly used for improving crop growth (Australian Bureau of Statistics, 2018). However, the
44 mobility, and thus plant availability, of fertiliser P can be significantly reduced by adsorption and
45 various precipitation reactions in soil (Coleman et al., 1960; Murrmann and Peech, 1969; Penn and
46 Camberato, 2019). In fact, less than 5% of applied P may be taken up in the year when it is applied
47 (Dorahy et al., 2005). However, over longer time frames it has been suggested that the uptake of
48 residual P can increase to over 70% (Syers et al., 2008; Dhillon et al., 2017), where climatic and
49 soil factors influence fertiliser efficiency. Band application of P fertilisers is often preferred as it
50 is more efficient than broadcast application, minimises the tie-up of P, provides early growth
51 stimulation and eliminates the adverse effects from concentrating the fertilizer too near the seed
52 (Randall and Hoelt, 1988). Determining the diffusion behaviour of banded P fertilisers in various
53 soil types can be used to evaluate new fertiliser formulations and to help optimise soil management
54 practices as higher P diffusion indicates that less fixation has occurred (e.g. Lombi et al., 2005).

55
56 To investigate fertiliser P diffusion in soil, past studies have typically collected and analysed soil
57 at varying distances (and incubation times) from the point of P fertiliser application. Various
58 methods have been used to make these measurements and are summarised by Degryse and
59 McLaughlin (2014). The same authors developed a high-resolution visualisation technique for P
60 fertiliser diffusion in soils using an iron (III) oxide impregnated paper. The iron (III) oxide
61 impregnated paper (P_i test) was first developed by Sissingh (1983) and modified by Menon et al.

62 (1989). In this test, iron (III) oxide impregnated paper was added to the CaCl₂ soil extraction then
63 eluted in an acidic solution and the amount of P measured. Degryse and McLaughlin (2014)
64 modified this technique by placing the iron oxide impregnated paper in direct contact with the soil
65 surface then visualising P distribution using a modified malachite green method. This method
66 provided very useful insights into the diffusion of P from several fertiliser formulations across a
67 range of soil types. The results were comparable to chemical extraction methods (0.5 mol/L CaCl₂)
68 where the soils were sampled in concentric circles around the granule. However, the visualisation
69 method produces images with varying colours due to the background colour of the malachite green
70 method. Also, the iron (III) oxide impregnated paper may be stained by soil particles, limiting the
71 precision of P measurements by this method. Other researchers have used this technique to
72 visualise the P diffusion of different fertilisers in soils, but not to accurately quantify P
73 concentrations at different distances from the granule (McLaren et al., 2016; Degryse et al., 2017;
74 Everaert et al., 2017; Andelkovic et al., 2018; Lustosa Filho et al., 2019).

75
76 High-resolution visualisation techniques have been used in biogeochemical sediment studies for a
77 number of years to interpret two-dimensional data obtained using passive sampler techniques
78 (Teasdale et al., 1999; Robertson et al., 2008; Pagès et al., 2011; Ding et al., 2013; Bennett et al.,
79 2015; Guan et al., 2015; Liu et al., 2020). The DGT (diffusive gradients in a thin-film) technique
80 (Davison and Zhang, 1994), combines a hydrogel diffusional layer and a binding layer that uses
81 mineral phases (including iron(III) oxide and zirconium hydroxide), resins or membranes to
82 accumulate solutes of interest to allow sensitive determination (Zhang et al., 1998; Ding et al.,
83 2013; Guan et al., 2015; Davison, 2016; Huang et al., 2016; Zhu et al., 2019). A related method,
84 the DET (diffusive equilibrium in a thin-film) passive sampler technique uses a single hydrogel

85 layer (Davison et al., 1991). Both passive sampler techniques colorimetric DET and DGT
86 techniques have been described for labile phosphate (PO₄-P), iron(II), sulfide and ammonium for
87 sediment studies (Teasdale et al., 1999; Pagès et al., 2011; Ding et al., 2013; Bennett et al., 2015;
88 Kankanamge et al., 2017; Metzger et al., 2019; Kankanamge et al., 2020; Liu et al., 2020). The
89 first study of two-dimensional DGT in soil was presented by Santner et al. (2012) using laser
90 ablation inductively coupled plasma mass spectrometry (LA-ICP-MS) to determine the
91 distribution of PO₄-P around plant roots on a hydrogel containing ferrihydrite. However, using
92 LA-ICP-MS can be quite expensive (\$50-100 per hour), time-consuming (measuring 8 cm² of a
93 sample in 4 hour with a scanning speed of 200 μm s⁻¹) (Santner et al., 2010; Kruse et al., 2015)
94 and, the PO₄-P binding capacity of a ferrihydrite gel layer is lower than other binding materials
95 (Bennett et al., 2010; Ding et al., 2010; Guan et al., 2015). More recently, Ding et al. (2013)
96 developed a colorimetric technique using DGT for measuring PO₄-P in sediment porewater.
97 However, this technique is limited by its slow processing time as a 5-day heat pre-treatment (80°C)
98 of binding layers is required and colour development requires gel incubation for 45 min at 35°C.

99

100 The aim of our study was to develop and evaluate a new and fast colorimetric DGT technique with
101 a thin diffusive layer and a high binding capacity to accurately visualise and quantify labile PO₄-
102 P concentrations in soils using Computer Imaging Densitometry (CID). The visualisation of data
103 can be a very effective way to engage and inform end users about the new fertiliser formulations
104 and the optimum soil management practices. Also, it was important to develop a DGT that was
105 easy to handle, could be manipulated without tearing, and could be prepared in various shapes and
106 sizes. For these reasons and for the first time, we prepared a membrane-based binding layers for
107 the 2D quantitative visualisation of phosphate diffusion from fertilisers in soil. Experiments were

108 carried out to: a) develop membrane-based zirconia (Zr)-oxide binding and diffusive gel layers
109 (Zr-oxide was chosen due to its high binding capacity (Ding et al., 2010; Ding et al., 2013; Guan
110 et al., 2015); b) determine the optimal reaction temperature and coloration time for the colorimetric
111 technique; c) compare the efficacy of the new colorimetric DGT technique to elution DGT
112 techniques; and, d) investigate the diffusion of phosphate away from granular P fertilisers in soils.

113

114 **2. Methodology**

115 2.1. Materials, reagents and solutions

116 AR grade chemicals reagents were used in all experiments and all solutions were prepared using
117 ultrapure deionised water (18.2 M Ω .cm, Milli-Q Advantage 10, Millipore). The detail of materials,
118 reagents and solutions used in this study are presented in Supporting Information (SI) **1.1**.

119

120 2.2. Gel layer preparation

121 2.2.1. Preparation of membrane-based diffusive gel and Zr-oxide binding gel

122 Membrane-based diffusive and binding gel layers were used for their structural integrity; a
123 requirement of these experiments was that the gel layers needed to be cut into different sizes and
124 easily manipulated without tearing.

125

126 The bis-acrylamide gel stock solution was prepared according to previous studies (Robertson et
127 al., 2008; Bennett et al., 2012). Membrane-based bis-acrylamide diffusive gels were then prepared
128 by soaking PES filter membranes (25 mm and 76 mm) in the bis-acrylamide gel stock solution for
129 10-15 s. The membranes were then placed flat between two plastic sheets (making sure to remove
130 air bubbles) and left to polymerise at room temperature for 40 min. The polymerised diffusive gels

131 were then rinsed three times with ultrapure deionised water within 24 h before storage. As a result,
132 diffusive gel discs of 0.2 mm thickness were obtained, which was measured using an
133 electronic stainless-steel micrometer (Mahr, TESA, Mitutoyo, Sylvac). The diffusive gel discs
134 were stored in 0.01 mol/L NaCl before deployment.

135
136 The Zr-oxide binding layers were prepared according to Guan et al. (2015) with some
137 modifications. Specifically, the membrane-based bis-acrylamide diffusive gel discs were
138 immersed in a solution of 32.2 g/L of $\text{ZrOCl}_2 \cdot 8\text{H}_2\text{O}$ for 2 h, followed by immersion in MES
139 monohydrate (10.66 g/L) for 40 min at pH 6.7 (pH adjusted using 0.1 mol/L NaOH). Precipitated
140 Zr-oxide binding gel discs of 0.2 mm thickness were obtained.

141
142 2.2.2. Preparation of staining gel
143 The bis-acrylamide staining gels (15 cm×20 cm) – on which the binding gels were placed after
144 DGT deployment – were prepared according to Bennett et al. (2012) and Pagès et al. (2011). The
145 staining gels were soaked in a colour reagent, which was prepared based on the standard
146 molybdate-ascorbic acid method (APHA P-E), for 1.5-2 h before use (Lin and Wu, 1996; Pagès et
147 al., 2011).

148
149 2.3. Assembly and validation of DGT with membrane-based binding layer

150 2.3.1. Assembly of solution and soil standard DGT samplers
151 In this study, two types of standard DGT sampler were used for the method development, including
152 solution DGT with an exposed surface area of 3.14 cm² and soil DGT with an exposed surface
153 area of 2.54 cm². The DGT samplers were assembled using three different layers, from top (i.e. in

154 contact with soil) to bottom: a 0.45 μm PES membrane filter (0.1 mm), a bis-acrylamide gel (0.2
155 mm) and a Zr-oxide binding gel (0.2 mm). To ensure the gel assembly did not move within the
156 DGT device, a 0.8 mm bis-acrylamide gel layer was placed under the Zr-oxide binding layer
157 followed by a plastic cap placed on the top layer.

158

159 2.3.2. DGT calculations

160 The DGT-measured concentration (C_{DGT} : $\text{ng/mL}=\mu\text{g/L}$) of $\text{PO}_4\text{-P}$ in solution and soil was
161 calculated from the accumulated analyte mass using the DGT equation (Eq. 1) (Zhang and
162 Davison, 1994),

163

$$C_{\text{DGT}} = \frac{M * \Delta g}{A * D * t} \quad (1)$$

164 where M is the accumulated mass of $\text{PO}_4\text{-P}$ during the deployment time (ng), Δg is the thickness
165 of the diffusive layer (cm), D is the diffusion coefficient for $\text{PO}_4\text{-P}$ through the diffusive layer
166 ($1.74 \times 10^{-6} \text{cm}^2/\text{s}$), t is the deployment time (s), and A is the area of the gel in contact with the
167 solution or soil (cm^2).

168

169 2.3.3. Mass accumulation over time and diffusion coefficient

170 Solution DGT devices were deployed in 10 L of 1 mg $\text{PO}_4\text{-P/L}$ solution with 0.01 mol/L NaNO_3 .
171 The solution was prepared 24 h before DGT deployment to allow the solution to equilibrate in the
172 container. DGT devices were deployed for 4, 8, 12, 24 and 48 h (n=5). 10 mL aliquots of the
173 phosphate solution were collected before the deployment and after the removal of DGT devices.

174 pH, electrical conductivity and temperature were also measured before the DGT devices were
175 deployed and after they are removed.

176

177 After removing the DGT probes from solutions, they were rinsed with deionised water and stored
178 at 4°C in sealed plastic bags until analysis. For the five DGT replicates deployed in 1 mg PO₄-P/L
179 solution, three were used for the colorimetric determination of PO₄-P concentrations (see section
180 2.4), and the other two were analysed using elution techniques. For the elution, DGT devices were
181 eluted with 0.5 mol/L NaOH using the reported elution efficiency of 96.2% (Guan et al., 2015),
182 then diluted with deionised water (1-100 times) before reactive phosphate analysis (molybdate-
183 ascorbic acid method) using a Skalar segmented flow analyser (Scan++, Skalar).

184

185 The diffusion coefficient, D , of PO₄-P from the membrane-based diffusive gel layer was based on
186 Eq. 2 (SI), which is determined from mass accumulation over time experiments as described
187 previously (Zhang and Davison, 1995).

188

189 2.4. Validation of the colorimetric method

190 2.4.1. Determining the optimum staining time and temperature

191 The membrane-based Zr-oxide binding layers, part of the DGT devices, were deployed in 10 mL
192 of 13 different PO₄-P concentrations (KH₂PO₄, Chem Supply), ranging from 0 to 50 mg/L for 24
193 h (n=6). After that, the membrane-based Zr-oxide binding layers were removed from solutions and
194 placed on staining gels to develop colour (see section 2.6). To determine the optimum staining
195 time, images were scanned after a 2 min reaction time, then every 3 min for up to 2 h. Two reaction
196 temperatures of 20°C (room temperature) and 40°C (using a laboratory oven, 5 °C higher than Ding
197 et al. (2013)) were selected, in order to determine the optimum temperature.

198

199 2.4.2. Calibration curve and binding capacity

200 Solution DGT devices were deployed in nine different PO₄-P concentrations, ranging from 0 to
201 6.9 mg/L in 10 L of 0.01 mol/L NaNO₃ solutions. The solutions were prepared 24 h before DGT
202 deployment. Five DGT devices were deployed in each concentration for 24 h. 10 mL of the
203 phosphate solution were collected before the DGT devices were deployed and after they were
204 removed. Additionally, pH, electrical conductivity and temperature were measured before the
205 DGT devices were deployed and after they are removed. After removing the DGT probes from
206 solutions, they were rinsed with deionised water. Among the five DGT samplers, three of them
207 were used for colorimetric development to determine the grayscale intensity (GSI) values by
208 placing the membrane-based Zr-oxide binding layers on staining gels for scanning. The other two
209 gels were analysed using elution techniques to measure the PO₄-P mass on the binding layers and
210 the eluents were measured by Scan++. A calibration curve was determined by plotting the
211 grayscale intensity values (n=3) versus the different PO₄-P concentrations (μg/cm²) measured
212 using the elution method (n=2). The calibration curve allowed us to determine the most suitable
213 PO₄-P concentrations for our subsequent experiments. This experiment also allowed us to
214 determine the binding capacity of Zr-oxide to be determined (see section 3.3).

215

216 2.5. DGT deployment in soils

217 2.5.1. Deployment in soils amended with P fertiliser

218 After validating the colorimetric technique, modified DGT devices were used to investigate the
219 diffusion of PO₄-P from a granular phosphate fertiliser in soil (Figure S1 in SI). Three different
220 Australian soils were used for this experiment: 1) a calcareous clay loam from South Australia
221 (SA), 2) a clay cropping soil from New South Wales (NSW) and 3) a clay ferrosol from

222 Queensland (QLD). The pH, EC, phosphate concentration, phosphorus buffering index (PBI), and
223 cation concentrations varied between each soil (Table S1).

224

225 In this experiment, much larger (76 mm diameter) membrane-based bis-acrylamide diffusive gel
226 layers and precipitated Zr-oxide binding layers were prepared. The experimental set-up was based
227 on the method described previously by Lombi et al. (2004 and 2005). Where 75 g (dry weight) of
228 each soil was weighed into a 76 mm diameter petri dish to give a soil density of 1.06 g/cm³ for the
229 SA soil, 1.02 g/cm³ for the QLD soil, and 1.29 g/cm³ for the NSW soil. Soils were brought to 80%
230 MWHC, using deionised water, then incubated for 24 h. Six petri dishes were prepared for each
231 soil, where two were used as a blank (no fertiliser added), and one P fertiliser granule added to
232 each of the other four dishes. The monoammonium phosphate (MAP) granule (55 ± 3 mg) with 11
233 mg of P per dish was placed on top and in the middle of the soil, then pushed down (5 mm) to half
234 the soil depth using a pin (Lombi et al., 2004; Lombi et al., 2005). Then the petri dishes were
235 sealed with parafilm and incubated for 35 days at 25°C.

236

237 After the incubation, the membrane-based bis-acrylamide diffusive layers (which were the same
238 size as the petri dish), were laid directly on top of the soil, followed by the Zr-oxide binding layer.
239 To ensure that there was no air gap between the soil and membrane-based bis-acrylamide diffusive
240 layers, and between the membrane-based bis-acrylamide diffusive layers and the Zr-oxide binding
241 layer the upturned lid of the petri dish was placed on top of the gel layers. This facilitated complete
242 contact between the soil and the gel layers and maintained the gel layer moisture for the 24 h
243 deployment time (Figure S1). Nine of the DGT samplers were analysed using the novel
244 colorimetric visualisation technique while the rest were measured using the elution and analysis

245 technique. The binding layers measured by the elution technique were sliced into four concentric
246 rings (centred on the fertiliser granule) using stainless steel cylinders with different diameters to
247 investigate the diffusion of $\text{PO}_4\text{-P}$ away from the fertiliser granule in the different soil types. The
248 ring diameters, from the innermost ring to the outermost, were 14, 30, 56, and 76 mm (Figures 2).

249

250 After removing the DGT from the petri dish, four concentric rings of soil – having the same
251 diameters as the sliced DGTs – were collected from the petri dish. The same cylinders were pushed
252 into the soil and the soil scooped out of each concentric ring using a plastic spatula. Soils were
253 then dried at 60°C for 5 d and the Colwell P extraction technique (Colwell, 1963) was used to
254 determine the $\text{PO}_4\text{-P}$ concentration in each soil ring. Briefly, 0.5 g of soil was extracted with 50
255 mL of 0.5 mol/L bicarbonate (NaHCO_3) in a soil:solution ratio of 1:100, then shaken on an end-
256 over-end shaker for 16 h. Phosphorus concentrations in the extractant were then measured using
257 Scan++.

258

259 Finally, the results provided by the colorimetric technique were compared to those obtained from
260 the standard elution technique and the Colwell P method. In addition, after DGT deployment, the
261 fertiliser granules were removed from the soil using tweezers and dried at 60°C for 5 days. Adhered
262 soil was gently removed using a brush and the granule weighed. The differences in $\text{PO}_4\text{-P}$ diffusion
263 from the fertiliser in the three soils were evaluated.

264

265 2.5.2. Deployment in unamended soils with low concentration of available P

266 Soil DGT devices were deployed in three contrasting soils collected from Western Australia; they
267 were named as Kalannie (sandy loam), Condering (silt) and Jennacubine (sandy). The soils
268 differed in their pH, phosphate buffering index (PBI), exchangeable iron and aluminium content,

269 and organic carbon content (Table S2). 50 g (dry weight) of each soil was weighed into a petri dish
270 (76 mm diameter) with three replicates per soil. 24 h before DGT deployment, deionised water
271 was added to each dish to bring the soil to its maximum water holding capacity (MWHC) (Mason
272 et al., 2008). Two DGT probes were deployed in each petri dish i.e. a total of six DGT probes were
273 deployed in each soil. After deployment for 24 h, the DGT devices were rinsed with deionised
274 water to remove any residual soil, then disassembled for analysis. One DGT from each petri dish
275 was analysed using the colorimetric technique, and the other analysed using the elution technique.
276 Results from the colorimetric method (C_{DGT-C}) and elution method (C_{DGT-E}) were then compared.

277

278 2.6. Image scanning to determine PO_4 -P concentration and distribution

279 Following 24 h deployment, the membrane-based Zr-oxide binding layers were placed on a 0.2
280 mm plastic spacer. The staining gels were laid on another 0.2 mm plastic spacer and excess reagent
281 was wiped off to ensure that clear images were taken by the scanner. Then, the staining gel was
282 placed on top of the membrane-based Zr-oxide binding layers to develop the blue colour. The
283 intensity of the blue colour was measured using a CanoScan 9000F Mark II scanner at a resolution
284 of 300 dpi, corresponding to a pixel size of $169 \times 169 \mu\text{m}$. The images were scanned for 26 minutes
285 at 20°C (room temperature). Then the scanned images of the coloured binding gels were formatted
286 using GIMP 2.8.22, and ImageJ 1.51K1 software was used to produce/calculate the grayscale
287 intensity in each Zr-oxide binding layer. All collected data were then analysed using Microsoft
288 Excel 2016. For each PO_4 -P concentration, the calibration curve was applied, the reaction time,
289 temperature and average grayscale intensity for three replicate discs were calculated.

290

291 To quantify the two-dimensional (2D) diffusion of PO₄-P away from the fertiliser granule in each
292 soil (SA, NSW, and QLD), GIMP 2.8.22 and ImageJ 1.51K1 software were used following the
293 procedure described by Kankanamge et al. (2020) with some modification as described in the **SI**
294 **1.4**.

295

296 **3. Results and discussion**

297 3.1. Optimum staining time and temperature

298 The results indicate that the colour intensity was stable after approximately 38 minutes at 20°C,
299 and 26 minutes at 40°C (Figures S2 and S3). As expected, the higher temperature increased the
300 reaction rate meaning colour development was more rapid at 40°C. According to Bennett *et al.*
301 (2012), the most appropriate staining time is when the grayscale intensity of each concentration
302 exceeds at least 80% of the highest intensity value during the colour development period, which
303 provides suitable colour development for scanning and also minimise diffusive relaxation.
304 Therefore, the optimal staining time was 26 minutes at 20°C and 20 minutes at 40°C, although we
305 note that if greater sensitivity is required these times can be extended. In the subsequent
306 experiments, 26 minutes at 20°C was selected as the preferred staining time and temperature.
307 Additionally, Ding et al. (2013) reported a significant edge effects after staining without heat
308 treatment where there was a gradual change of the blue colour on the blank gel layer from the
309 sliced lateral edge to the center. Our results also show this edge effect, but the effect was not
310 significant (Figures S3 and S4). Our study shows that the differences between the center and the
311 lateral edge are less than 12 GSI while the difference was more than 50 GSI in Ding's study without
312 heat treatment. To avoid edge effects, the edge of the images should not be captured during image
313 and data processing.

314 3.2. Mass accumulation of labile P over time and determination of the diffusion coefficient

315 The mass of PO₄-P adsorbed to the membrane-based Zr-oxide binding layer increased linearly
316 over the 48 h deployment with an R² of 0.98 (Figure S5). Using Eq 2 from SI, the effective
317 diffusion coefficient of 1.74×10^{-6} cm²/s for PO₄-P was obtained from the linear regression line
318 at 21°C. The diffusion coefficient of PO₄-P from this study was only 32% of the diffusion
319 coefficient determined using an open diffusive gel layer (polyacrylamide with agarose cross-
320 linker) from DGT Research (5.42×10^{-6} cm²/s at 21°C) (Zhang et al., 1998; Price et al., 2013).
321 This was anticipated because our study used a 0.45 µm membrane-based bis-acrylamide diffusive
322 layer which further reduced the pore size of the diffusive layer. Shiva et al. (2015) showed that the
323 diffusion coefficients of oxyanions when using a bis-acrylamide diffusive gel layer was between
324 0.66 and 0.77 the diffusion coefficients of the open diffusive gel layer. This calculated DGT
325 diffusion coefficient, was corrected for temperature as appropriate using the Stokes-Einstein
326 equation (Zhang and Davison, 1995), and was used for all calculations in this study.

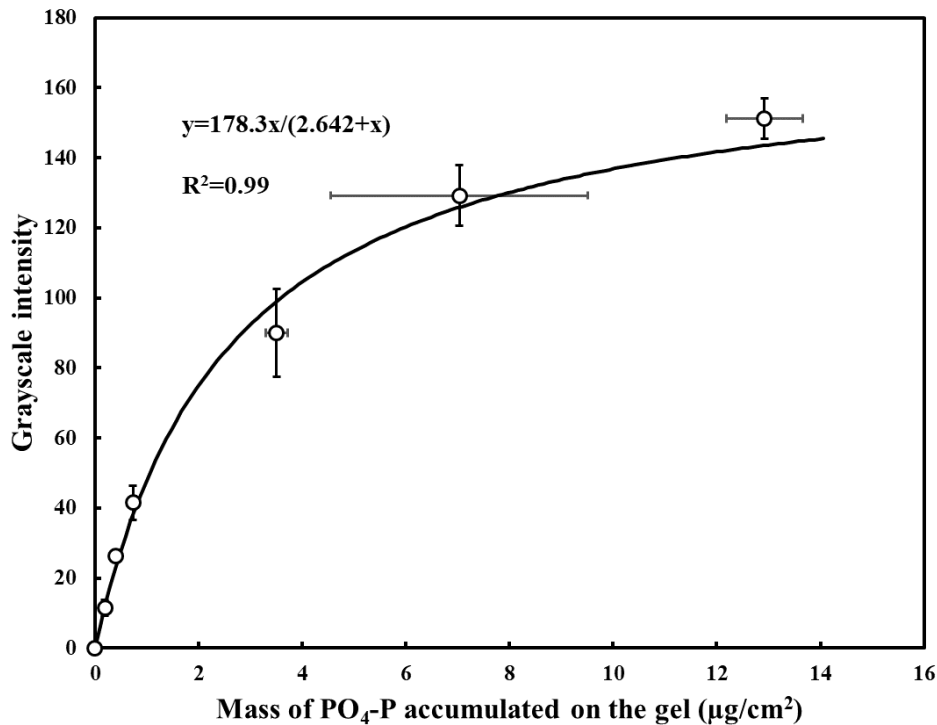
327

328 3.3. Calibration curve and determination of the binding capacity

329 In this study, a calibration curve was determined following 24 h DGT deployment in PO₄-P
330 solutions ranging in concentration from 0 to 6.9 mg/L. The average greyscale value for blank gels
331 (n=3) was 41.6 ± 1.10 , which is equal to 3.2 µg/L PO₄-P. The grayscale intensity values at each
332 PO₄-P concentration were determined by the colorimetric method (n=3) with the blank value
333 subtracted. A calibration curve was determined by plotting the grayscale intensity values versus
334 the different PO₄-P mass densities (µg/cm²) measured using the elution and analysis method (n=2).

335

336 A non-linear calibration curve (Hyperbola, Single Rectangular 2 Parameter) was achieved with
337 an R^2 of 0.99 (Figure 1). This curve is comparable to calibration curves that are presented for other
338 colorimetric DGT techniques (Teasdale et al., 1999; Robertson et al., 2008; Ding et al., 2013).
339 This calibration curve was used to calculate all subsequent $\text{PO}_4\text{-P}$ concentrations (section 3.3-3.6),
340 and the limit of detection of $\text{PO}_4\text{-P}$ (LOD = three times the standard deviation of the blank gel
341 layers) which was $0.05 \mu\text{g PO}_4\text{-P /cm}^2$ ($n=3$). This value corresponds to a LOD of $10.1 \mu\text{g/L}$ for
342 the colorimetric technique following 24 h DGT deployment using a diffusive layer of 0.3 mm
343 thickness at 21°C . The LOD for the colorimetric technique is approximately four times lower than
344 that ($40 \mu\text{g/L}$) reported by Ding et al. (2013), and only slightly higher than that ($6.8 \mu\text{g/L}$) presented
345 by Pagès et al. (2011). The LOD of our colorimetric method is higher than that for the elution
346 technique ($1.7 \mu\text{g/L}$), while the LOD from the elution technique is similar to other LODs for $\text{PO}_4\text{-P}$
347 P (from 0.04 to $1.2 \mu\text{g/L}$) determined for various binding materials, such as ferrihydrite, Metsorb,
348 Zr-oxide, Magnesium Carbonate based on 24 h deployment (Zhang et al., 1998; Panther et al.,
349 2010; Guan et al., 2015; Fa-Zhi et al., 2016). Most importantly, the colorimetric technique LOD
350 of the current study is low enough to measure $\text{PO}_4\text{-P}$ concentrations in most natural waters,
351 sediment and soil. To further improve sensitivity, modifications can be made such as using shorter
352 staining times or applying different colour channels during the scanning analysis stage (Bennett et
353 al., 2012).
354



355
 356 **Figure 1.** Plot of grayscale intensity (n=3) versus the mass of PO₄-P accumulated on the gel
 357 (µg/cm²) measured by the elution method (n=2) using a 26 min staining time and at 20°C. The
 358 error bars indicate the standard deviation of the mean (SD for the grayscale intensity ranged from
 359 1.1 to 19 and SD for the mass of PO₄-P accumulated on the gel ranged from 0 to 3.3 µg/cm²). The
 360 calibration line was fitted using Sigma Plot 11.0 using the non-linear curve (Hyperbola, Single
 361 Rectangular 2 Parameter) with the highest R².

362
 363 The binding capacity of the membrane-based Zr-binding layer was also determined by the
 364 colorimetric method using a 24 h DGT deployment across a wide range of PO₄-P equivalent
 365 concentration solutions (0, 0.028, 0.052, 0.11, 0.60, 1.10, 2.20, 3.90 and 6.90 mg/L). Figure S6
 366 shows that the accumulated mass in the binding layer, measured by the colorimetric method,
 367 increased non-linearly and plateaued around 13 µg/cm² PO₄-P, whereas the value measured by the
 368 elution technique continued to increase and reached 18.2 µg/cm² (Figure S7). The slightly lower

369 binding capacity determined by the colorimetric method is mainly due to the saturation effects in
370 the colorimetric method. Additionally, the capacity of using the colorimetric method for the
371 membrane-based Zr-oxide binding layer for PO₄-P at 13 µg/cm² corresponds to PO₄-P
372 concentrations of 2.5 mg/L for 24 h deployment with the diffusion coefficient of 1.74×10^{-6} cm²/s.
373 For the elution method, an accumulation of 18.2 µg/cm² corresponds to PO₄-P concentrations of
374 3.5 mg/L based on the same deployment time and diffusion coefficient. This binding capacity is
375 lower than the capacity obtained by both Guan et al. (2015) (65 µg/cm²) and Ding et al. (2013) (23
376 µg/cm²). One reason for the lower binding capacity in the current study is that our membrane-
377 based binding gel was two times thinner than those used by Guan et al. (2015) and Ding et al.
378 (2013). For thicker binding gel layers, the phosphate may not just be bound on the surface, but
379 also retained to a greater extent inside the gel, leading to a higher capacity. Again, other options,
380 such as using shorter staining times or applying different colour channels during the scanning
381 analysis stage, can be applied to modify this calibration curve to increase the upper measurement
382 limits as required (Bennett et al., 2012). Overall, the binding capacity of our current study is still
383 higher than values previously reported for precipitated ferrihydrite gel (approximately 7.0 µg/cm²)
384 (Santner et al., 2010) and Metsorb gel layer (11.7 µg/cm²) (Panther et al., 2010, 2011). In the study
385 of Degryse and McLaughlin (2014), there was a negative relationship between the median color
386 value and the P solution concentration, which was different from our technique. This is caused by
387 the different procedures when processing the image; we used 256 (highest GSI value) to subtract
388 the received GSI values after scanning (Kankanamge et al., 2020) while Degryse and McLaughlin
389 (2014) did not use this approach. However, this does not affect the interpretation of the results.
390 The visualization technique from Degryse and McLaughlin (2014) could determine PO₄-P

391 concentrations in CaCl₂ solution to approximately 100 mg/L based on a 30 min deployment time
392 while our technique was able to measure up to 120 mg/L PO₄-P for the same deployment time.

393

394 3.4. Validation of colorimetric technique for phosphate measurement in soils with low P

395 The colorimetric visualisation and elution Zr-oxide DGT techniques were used to obtain the PO₄-
396 P concentrations in three soil samples collected from Western Australia, named Kalannie (K),
397 Condering (C) and Jennacubine (J) (Table S3). Soils K and C had much lower PO₄-P
398 concentrations, as determined using both techniques, than soil J. The C_{DGT-C}/C_{DGT-E} ratios were
399 found to be 0.66, 0.86 and 0.90 for soils K, C and J, respectively. There was close agreement
400 between two of the three soils, although the colorimetric visualisation did slightly underestimate
401 the DGT-labile P concentrations. The lower ratio for soil K is most likely due to the relatively low
402 PO₄-P concentration and some heterogeneity in the soil. Additionally, the PO₄-P concentrations in
403 K and C soils were close to the LOD (10.1 µg/L) of the colorimetric technique, and these levels
404 are still important for the interpretation of DGT for PO₄-P measurements as not all the soils have
405 high PO₄-P concentrations and increasing the deployment time can address this issue in future
406 studies. Although the ratio was lower for soil K, the PO₄-P concentrations measured by the two
407 techniques were not significantly different due to the variance in elution values (Independent T-
408 test, p>0.05). Overall, the colorimetric technique provided reliable measurements of PO₄-P in soils,
409 and further detailed investigations should be carried out to investigate the effect of soil
410 composition and phosphate concentrations on the colorimetric technique. However, the main
411 purpose of this study was to develop a two-dimensional visualisation study for soil fertiliser tests
412 and these results confirm that the colorimetric technique can provide accurate data, especially at
413 higher concentrations.

414

415 3.5. Two-dimensional measurement of phosphate diffusion in fertilised soils and comparison of

416 DGT_{-colorimetric}, DGT_{-elution} and Colwell P techniques

417 Colorimetric DGT devices were used to investigate the diffusion of PO₄-P away from a MAP

418 fertiliser granule in three Australian soils (SA, QLD and NSW). After scanning the colorimetric

419 gels from the three fertilised soils at the optimum staining time and temperature, the images were

420 processed by GIMP and ImageJ software according to Kankanamge et al. (2020) and the two-

421 dimensional measurement of PO₄-P concentration in the binding layers were obtained (Figure 2).

422 Phosphate concentrations in the 2D-images ranged from 10.1 µg/L (white) to greater than or equal

423 to 2000 µg/L (black) (Figure 2). Phosphate was relatively immobile in the calcareous SA soil,

424 slightly more mobile in the QLD soil, and had the greatest mobility in the NSW soil. For both the

425 SA and QLD soils, movement of potentially available P was limited to 15 mm from the fertiliser

426 application point, with PO₄-P concentrations less than 50 µg/L at distances between 15 and 38 mm

427 from the granule for both soils (Figure 2i-iv). For the NSW soil, potentially available P diffused

428 further from the granule, with hotspots exceeding 2000 µg/L between 28 and 38 mm from the

429 granule in more than one area (Figure 2 vi). Only one sample (Figure 2 iv), showed a relatively

430 uniform high PO₄-P concentration within 7 mm from the granule which was most likely due to

431 direct contact between the fertiliser granule and the DGT gel layers. In this study, we tried to avoid

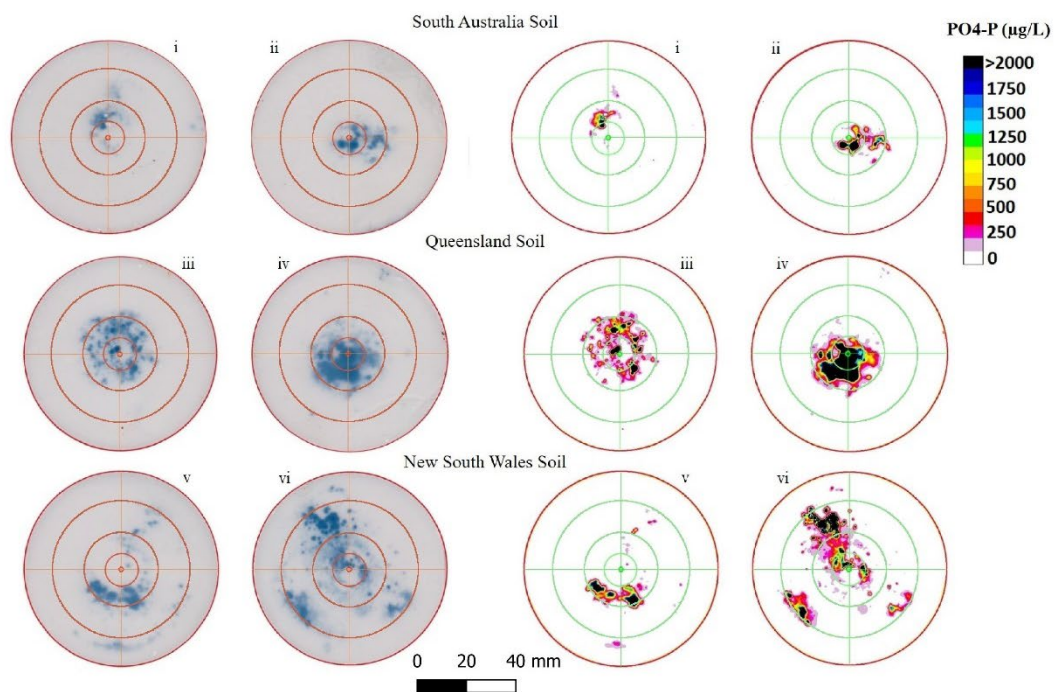
432 direct contact between the DGT gel layers and the fertiliser granule to prevent internal diffusion

433 of P within the gel layer. Internal diffusion can occur when very high concentrations of PO₄-P bind

434 to the Zr-oxide binding layer (e.g. from direct contact with the P fertiliser granule) and result in an
435 overestimation of PO₄-P diffusion.

436

437 These data demonstrate how two-dimensional visualisation measurements contribute to a clearer
438 understanding of the effect of soil type on PO₄-P diffusion and can visually demonstrate the
439 heterogeneity of P diffusion. Any issues with DGT deployment also become readily apparent, such
440 as in Figure 2iv.



441

442 **Figure 2.** On the left, a picture of the binding layer after 26 minutes of staining time at 20°C. Two
443 replicates of each of the three different soils were analysed. On the right, 2D-images obtained from
444 the scanned pictures on the left. The colour scale indicates the value for the phosphate
445 concentration in the binding layer (μg/L) determined by the colorimetric technique. The smallest
446 circles in the centre of binding layers and 2D images show the fertiliser application point. The

447 concentric circles surrounding this point (shown in red on the binding layers, and green on the 2D
448 images) indicate the distance from the fertiliser application point where the gels were sliced. These
449 circles have diameters of 14, 30, 56, and 76 mm, from the inner most ring to the outermost ring.

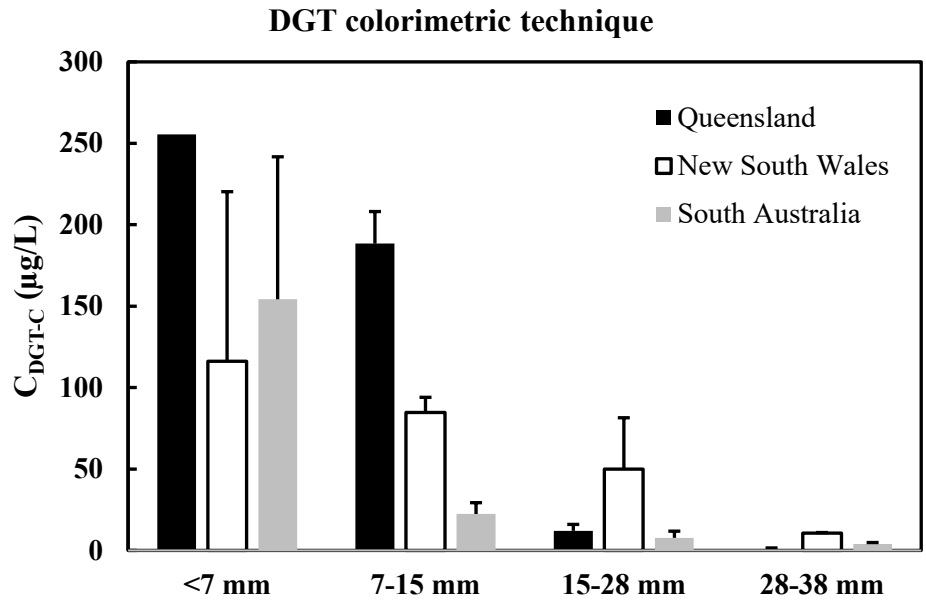
450

451 Regarding the $\text{PO}_4\text{-P}$ diffusion within the soils and neglecting the $\text{PO}_4\text{-P}$ concentration within 14
452 mm from the granule due to the high amount of variance between replicates, the three techniques
453 (DGT colorimetric, DGT elution, and Colwell P) gave very similar results. The qualitative trends
454 in $\text{PO}_4\text{-P}$ distribution were the same among all methods for all treatments (Figures 2 and 3), i.e.
455 diffusion of $\text{PO}_4\text{-P}$ away from the fertiliser granule increased as follows: SA < QLD < NSW.
456 Labile P concentrations measured colorimetrically ($C_{\text{DGT-C}}$) were compared to those measured
457 using the standard elution technique ($C_{\text{DGT-E}}$). Independent t-test results from Table S4 showed
458 that most $\text{PO}_4\text{-P}$ values determined from the DGT colorimetric and elution measurements were not
459 significantly different ($p>0.05$) with only one exception which was the value between 7 and 15
460 mm from the granule of QLD soil ($P=0.015$). This was most likely caused by direct contact
461 between the fertiliser granule and the DGT gel layers, leading to the high $\text{PO}_4\text{-P}$ concentration in
462 that area.

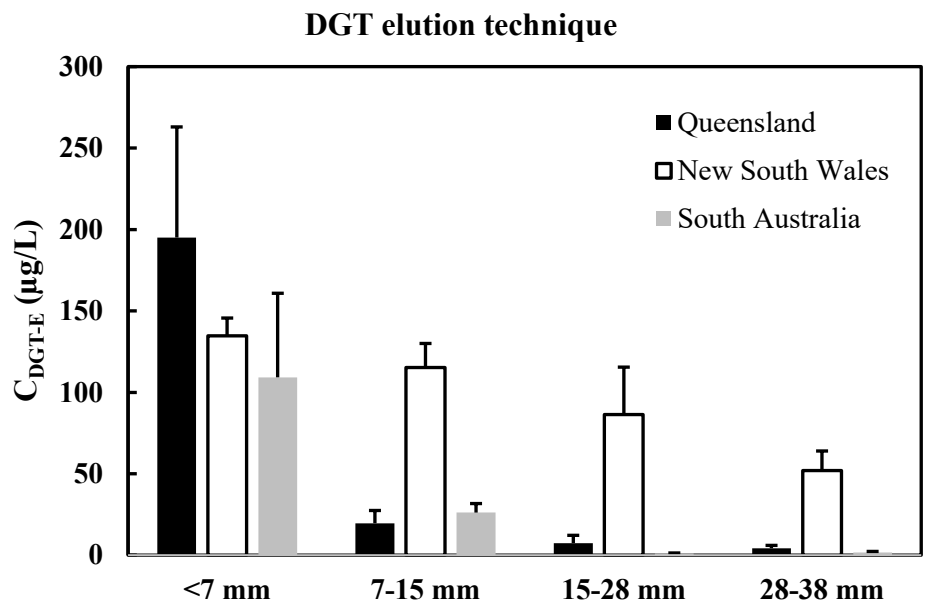
463

464 Overall, the DGT colorimetric method quantified analogous $\text{PO}_4\text{-P}$ concentrations to the DGT
465 elution technique. Furthermore, both techniques demonstrated similar patterns of $\text{PO}_4\text{-P}$ diffusion.
466 Conversely, the Colwell P method estimated much higher $\text{PO}_4\text{-P}$ concentrations for the SA soil
467 compared to the two DGT techniques. Critical Colwell P concentrations are affected by the ability
468 of the soil to adsorb P as the Colwell P test measures less available P as well as readily available
469 P. This is because using bicarbonate as the extractant can remove large amounts of phosphate that
470 are fixed to aluminium and calcium particles contained in the soil (Mason et al., 2010).

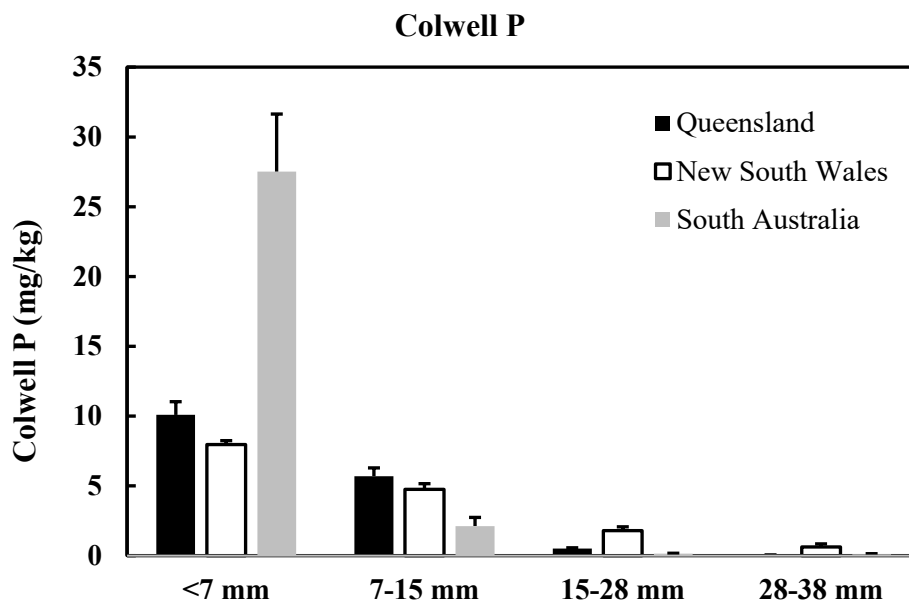
471 Additionally, it has been shown that Colwell P is not a good predictor of available P in calcareous
472 soils (Bertrand et al., 2003). Therefore, the Colwell P measurements may overestimate the true
473 concentration of PO₄-P in the SA soil, which had a high CaCO₃ content.



474



475



476

477 **Figure 3.** Phosphate concentration ($\mu\text{g/L}$ and mg/kg) determined by the DGT colorimetric, elution
 478 technique and Colwell P method in three different soils within different distance from the granule
 479 (Queensland, New South Wales and South Australia). The standard error was also plotted ($n=2$
 480 for the DGT colorimetric and elution technique, $n=4$ for Colwell P method). For the DGT
 481 colorimetric method, the value from <7 mm of QLD soil which is affected by the direct contact of
 482 the fertiliser was excluded.

483

484 3.6 Fertiliser dissolution in different soil types

485 Following the 35-day incubation – and immediately after DGT collection – MAP granules were
 486 extracted from the petri dishes and weighed. There was incomplete dissolution of MAP in all three
 487 soils after the incubation; however, there were differences in the mass decrease of granules
 488 between soils. In the QLD and NSW soils, MAP granules decreased by 74% (41 mg) and 76% (42
 489 mg), respectively, whereas in the SA soil, MAP only decreased in mass by 57% (31 mg) (Table
 490 S5). Therefore, as suggested by Lombi et al. (2004) who performed similar diffusion experiments,

491 the large amount of PO₄-P remaining within 14 mm of the QLD soil can be explained by a slower
492 rate of P diffusion compared to that in the NSW soil. In the SA soil, PO₄-P was also confined
493 within 14 mm, but in this case most likely due to the low dissolution rate of the MAP granule itself
494 and the low rate of P diffusion which can be attributed to soil properties. When the fertiliser granule
495 is initially added to the SA soil, the water drawn to the granule contains Ca²⁺, which can precipitate
496 P (Hettiarachchi et al., 2006). Due to the high concentration of P in the fertosphere (the volume of
497 soil around the granule), precipitation reactions dominate initially (Hettiarachchi et al., 2006).
498 Then, as P moves away from the granule and the concentration of P in soil solution decreases,
499 adsorption becomes the dominant process.

500

501 3.7 Effect of soil properties on PO₄-P diffusion away from fertiliser granules

502 The advantage of the DGT method is that compared to other techniques such as Colwell P, it is
503 suitable for a range of soil types. In addition, DGT compares more favourably than Colwell P in
504 relation to plant available P (Mason et al., 2010; Mason et al., 2013). Phosphate diffusion is largely
505 controlled by soil properties, specifically soil pH, presence of CaCO₃, and the concentration of
506 Al/Fe oxides. These properties also influence the soil's PBI. The QLD and SA soils both had a
507 moderate PBI (210 and 180, respectively) while the NSW soil had a low PBI of 73. High PBI
508 values indicate that the soil can quickly bind P. In soils with a low PBI, applied P is generally more
509 labile in the short term as the soil has a limited ability to bind P. The soil properties that influence
510 PBI (pH, CaCO₃, Al/Fe oxides), can also explain the differences in P diffusion observed in the
511 current study. Our results correlate well with the PBI values in that PO₄-P was most labile and

512 diffused further in the NSW soil; the soil with the lowest PBI. While for the QLD and SA soils
513 with high PBI, the $\text{PO}_4\text{-P}$ was less labile and the diffusion was lower.

514

515 When MAP dissolves in soil, the pH of the fertosphere soil solution becomes moderately acidic.
516 For this reason, MAP is advantageous in neutral and alkaline soils. However, in the presence of
517 Ca, P is rapidly removed from the soil solution. In calcareous alkaline soils, such as the SA soil
518 (pH 8.5, 36% CaCO_3 equivalent), orthophosphate ions can rapidly precipitate with Ca when the
519 soil solution concentration of PO_4^{3-} exceeds the solubility products for Ca-P solid phases (Freeman
520 and Rowell, 1981; Lindsay, 1979); effectively immobilising P. Therefore, this explains the limited
521 diffusion of P away from the fertiliser granule in the current study (Figures 2 and 3). In the acidic
522 QLD soil (pH=5.0), P fixation can also explain the limited diffusion of $\text{PO}_4\text{-P}$ away from the
523 fertiliser granule. However, for this soil, precipitation of P with Fe and Al oxides is the most likely
524 fixation mechanism. In the fertosphere of non-calcareous soils, precipitation of Al-P minerals
525 dominates as shown by Meyer et al. (2020). Using synchrotron-based X-ray absorption near edge
526 structure (XANES) analysis the authors found that when granular MAP was applied to an acidic
527 Tenosol, Al-P minerals such as taranakite, and absorbed P were the dominant P species. Finally,
528 P diffusion was greatest in the relatively neutral NSW soil (pH=7.4) not only because soil pH was
529 favourable for MAP dissolution, but also because precipitation and absorption reactions that act to
530 limit $\text{PO}_4\text{-P}$ diffusion were less prevalent. Specifically, Ca-P precipitation was less likely because
531 CaCO_3 was not detected in the soil, and, fixation by Al was reduced as exchangeable Al contributed
532 <0.1% to the soil's cation exchange capacity (CEC).

533

534

535

536 **4. Conclusion**

537 The novel colorimetric technique based on precipitated membrane-based Zr-oxide DGT was
538 developed. The optimal staining temperature and time were 20°C (room temperature) and 26
539 minutes. The new colorimetric technique was not only easier to perform without the need for any
540 pre-treatment of the binding gel layers and heating during scanning, but was also able to provide
541 faster results than the colorimetric technique developed by Ding et al. (2013). This makes the
542 technique more suitable for in-field applications. The technique was able to measure phosphate
543 concentration up to 2.5 mg/L for a 24-hour deployment with a detection limit of 10.1 µg/L. Due
544 to the relatively high capacity of the precipitated Zr-oxide binding layer, it was possible to measure
545 labile phosphate in a range of contrasting soils. The relatively low LOD will also allow for the
546 measurement of phosphate in most waters, sediments and soils. The phosphate values measured
547 by the colorimetric technique were similar to the values determined by the elution technique.
548 Additionally, it has been shown that the new colorimetric technique can be used to visualise the
549 diffusion of labile phosphate in soil types. This makes it possible to investigate the diffusion of
550 potentially available phosphate from conventional and novel fertilisers, which can then be
551 correlated with the plant uptake of P. Furthermore, the visualisation of data can be a very effective
552 way to engage and inform end-users about novel fertiliser formulations and how to optimise soil
553 management practices.

554

555 **Acknowledgments**

556 The authors would like to thank UniSA STEM for providing support to David Macias Arias's for
557 his Master study. We also thank Nutrient Advantage for soil characterisation. The authors also like

558 to honour the contribution of Professor Peter Teasdale to this manuscript. Professor Peter Teasdale
559 passed away during the revision of the manuscript, and this is a tough time for the team and his
560 family. Peter was a loving family man, a talented researcher and a great mentor. This warm and
561 kind man will be greatly missed by his family, friends, colleagues and students. His strong sense
562 of integrity and desire for scientific truth will continue to inspire other researchers.

563

564 **References**

- 565 Australian Bureau of Statistics, 2018. Land Management and Farming in Australia, 2016-17.
566 Andelkovic, I.B., Kabiri, S., Tavakkoli, E., Kirby, J.K., McLaughlin, M.J., Losic, D., 2018. Graphene oxide-Fe
567 (III) composite containing phosphate—A novel slow release fertilizer for improved agriculture
568 management. *Journal of cleaner production* 185, 97-104.
569 Bennett, W.W., Teasdale, P.R., Panther, J.G., Welsh, D.T., Jolley, D.F., 2010. New diffusive gradients in a
570 thin film technique for measuring inorganic arsenic and selenium (IV) using a titanium dioxide based
571 adsorbent. *Analytical Chemistry* 82, 7401-7407.
572 Bennett, W.W., Teasdale, P.R., Welsh, D.T., Panther, J.G., Jolley, D.F., 2012. Optimization of colorimetric
573 DET technique for the in situ, two-dimensional measurement of iron (II) distributions in sediment
574 porewaters. *Talanta* 88, 490-495.
575 Bennett, W.W., Welsh, D.T., Serriere, A., Panther, J.G., Teasdale, P.R., 2015. A colorimetric DET technique
576 for the high-resolution measurement of two-dimensional alkalinity distributions in sediment porewaters.
577 *Chemosphere* 119, 547-552.
578 Coleman, N., Thorup, J.T., Jackson, W., 1960. Phosphate-sorption Reactions That Involve Exchangeable
579 A1. *Soil Science* 90, 1-7.
580 Colwell, J., 1963. The estimation of the phosphorus fertilizer requirements of wheat in southern New
581 South Wales by soil analysis. *Australian Journal of Experimental Agriculture* 3, 190-197.
582 Davison, W., 2016. Diffusive gradients in thin-films for environmental measurements. Chapter 1
583 Introduction to DGT. Cambridge University Press.
584 Davison, W., Grime, G., Morgan, J., Clarke, K., 1991. Distribution of dissolved iron in sediment pore waters
585 at submillimetre resolution. *Nature* 352, 323-325.
586 Davison, W., Zhang, H., 1994. In situ speciation measurements of trace components in natural waters
587 using thin-film gels. *Nature* 367, 546-548.
588 Degryse, F., Baird, R., Da Silva, R.C., McLaughlin, M.J., 2017. Dissolution rate and agronomic effectiveness
589 of struvite fertilizers—effect of soil pH, granulation and base excess. *Plant and soil* 410, 139-152.
590 Degryse, F., McLaughlin, M.J., 2014. Phosphorus diffusion from fertilizer: visualization, chemical
591 measurements, and modeling. *Soil Science Society of America Journal* 78, 832-842.
592 Dhillon, J., Torres, G., Driver, E., Figueiredo, B., Raun, W.R., 2017. World phosphorus use efficiency in
593 cereal crops. *Agronomy Journal* 109, 1670-1677.
594 Ding, S., Wang, Y., Xu, D., Zhu, C., Zhang, C., 2013. Gel-based coloration technique for the submillimeter-
595 scale imaging of labile phosphorus in sediments and soils with diffusive gradients in thin films.
596 *Environmental science & technology* 47, 7821-7829.

597 Ding, S., Xu, D., Sun, Q., Yin, H., Zhang, C., 2010. Measurement of dissolved reactive phosphorus using the
598 diffusive gradients in thin films technique with a high-capacity binding phase. *Environmental science &*
599 *technology* 44, 8169-8174.

600 Dorahy, C., Rochester, I., Blair, G., 2005. Response of field-grown cotton (*Gossypium hirsutum* L.) to
601 phosphorus fertilisation on alkaline soils in eastern Australia. *Soil Research* 42, 913-920.

602 Everaert, M., Degryse, F., McLaughlin, M.J., De Vos, D., Smolders, E., 2017. Agronomic effectiveness of
603 granulated and powdered P-exchanged Mg–Al LDH relative to struvite and MAP. *Journal of agricultural*
604 *and food chemistry* 65, 6736-6744.

605 Fa-Zhi, X., Ting-Ting, H., Hao-Han, F., Xuan, L., Xian-Biao, W., SHENG, D.-D., Hai-Bin, L., Xue-Chun, W., Zhi-
606 Yong, X., 2016. Basic Magnesium Carbonate-Based DGT Technique for in situ Measurement of Dissolved
607 Phosphorus in Eutrophic Waters. *Chinese Journal of Analytical Chemistry* 44, 965-969.

608 Guan, D.-X., Williams, P.N., Luo, J., Zheng, J.-L., Xu, H.-C., Cai, C., Ma, L.Q., 2015. Novel precipitated
609 zirconia-based DGT technique for high-resolution imaging of oxyanions in waters and sediments.
610 *Environmental science & technology* 49, 3653-3661.

611 Hettiarachchi, G.M., Lombi, E., McLaughlin, M.J., Chittleborough, D., Self, P., 2006. Density changes
612 around phosphorus granules and fluid bands in a calcareous soil. *Soil Science Society of America Journal*
613 70, 960-966.

614 Huang, J., Bennett, W.W., Welsh, D.T., Li, T., Teasdale, P.R., 2016. “Diffusive gradients in thin films”
615 techniques provide representative time-weighted average measurements of inorganic nutrients in
616 dynamic freshwater systems. *Environmental science & technology* 50, 13446-13454.

617 Kankanamge, N.R., Bennett, W.W., Teasdale, P.R., Huang, J., Welsh, D.T., 2017. Comparing in situ
618 colorimetric DET and DGT techniques with ex situ core slicing and centrifugation for measuring ferrous
619 iron and dissolved sulfide in coastal sediment pore waters. *Chemosphere* 188, 119-129.

620 Kankanamge, N.R., Bennett, W.W., Teasdale, P.R., Huang, J., Welsh, D.T., 2020. A new colorimetric DET
621 technique for determining mm-resolution sulfide porewater distributions and allowing improved
622 interpretation of iron (II) co-distributions. *Chemosphere* 244, 125388.

623 Kruse, J., Abraham, M., Amelung, W., Baum, C., Bol, R., Kühn, O., Lewandowski, H., Niederberger, J.,
624 Oelmann, Y., Rügner, C., 2015. Innovative methods in soil phosphorus research: A review. *Journal of plant*
625 *nutrition and soil science* 178, 43-88.

626 Lin, S.H., Wu, C.L., 1996. Removal of nitrogenous compounds from aqueous solution by ozonation and ion
627 exchange. *Water Research* 30, 1851-1857.

628 Liu, L., Tang, W., Huang, J., Teasdale, P.R., Shu, L., Zhang, H., 2020. In situ, high-resolution measurement
629 of labile phosphate in sediment porewater using the DET technique coupled with optimized imaging
630 densitometry. *Environmental Research* 191, 110107.

631 Lombi, E., McLaughlin, M., Johnston, C., Armstrong, R., Holloway, R., 2004. Mobility and lability of
632 phosphorus from granular and fluid monoammonium phosphate differs in a calcareous soil. *Soil Science*
633 *Society of America Journal* 68, 682-689.

634 Lombi, E., McLaughlin, M.J., Johnston, C., Armstrong, R., Holloway, R., 2005. Mobility, solubility and lability
635 of fluid and granular forms of P fertiliser in calcareous and non-calcareous soils under laboratory
636 conditions. *Plant and Soil* 269, 25-34.

637 Lustosa Filho, J.F., Barbosa, C.F., da Silva Carneiro, J.S., Melo, L.C.A., 2019. Diffusion and phosphorus
638 solubility of biochar-based fertilizer: Visualization, chemical assessment and availability to plants. *Soil and*
639 *Tillage Research* 194, 104298.

640 Mason, S., Hamon, R., Zhang, H., Anderson, J., 2008. Investigating chemical constraints to the
641 measurement of phosphorus in soils using diffusive gradients in thin films (DGT) and resin methods.
642 *Talanta* 74, 779-787.

643 Mason, S., McNeill, A., McLaughlin, M.J., Zhang, H., 2010. Prediction of wheat response to an application
644 of phosphorus under field conditions using diffusive gradients in thin-films (DGT) and extraction methods.
645 *Plant and soil* 337, 243-258.

646 Mason, S.D., McLaughlin, M.J., Johnston, C., McNeill, A., 2013. Soil test measures of available P (Colwell,
647 resin and DGT) compared with plant P uptake using isotope dilution. *Plant and soil* 373, 711-722.

648 McLaren, T.I., McLaughlin, M.J., McBeath, T.M., Simpson, R.J., Smernik, R.J., Guppy, C.N., Richardson, A.E.,
649 2016. The fate of fertiliser P in soil under pasture and uptake by subterranean clover—a field study using
650 33 P-labelled single superphosphate. *Plant and Soil* 401, 23-38.

651 Menon, R., Hammond, L., Sissingh, H., 1989. Determination of plant - available phosphorus by the iron
652 hydroxide - impregnated filter paper (Pi) soil test. *Soil Science Society of America Journal* 53, 110-115.

653 Metzger, E., Barbe, A., Cesbron, F., de Chanvalon, A.T., Jauffrais, T., Jézéquel, D., Mouret, A., 2019. Two-
654 dimensional ammonium distribution in sediment pore waters using a new colorimetric diffusive
655 equilibration in thin-film technique. *Water research X* 2, 100023.

656 Murrmann, R., Peech, M., 1969. Effect of pH on labile and soluble phosphate in soils. *Soil Science Society
657 of America Journal* 33, 205-210.

658 Pagès, A., Teasdale, P.R., Robertson, D., Bennett, W.W., Schäfer, J., Welsh, D.T., 2011. Representative
659 measurement of two-dimensional reactive phosphate distributions and co-distributed iron (II) and sulfide
660 in seagrass sediment porewaters. *Chemosphere* 85, 1256-1261.

661 Panther, J.G., Teasdale, P.R., Bennett, W.W., Welsh, D.T., Zhao, H., 2010. Titanium dioxide-based DGT
662 technique for in situ measurement of dissolved reactive phosphorus in fresh and marine waters.
663 *Environmental science & technology* 44, 9419-9424.

664 Panther, J.G., Teasdale, P.R., Bennett, W.W., Welsh, D.T., Zhao, H., 2011. Comparing dissolved reactive
665 phosphorus measured by DGT with ferrihydrite and titanium dioxide adsorbents: Anionic interferences,
666 adsorbent capacity and deployment time. *Analytica chimica acta* 698, 20-26.

667 Penn, C.J., Camberato, J.J., 2019. A critical review on soil chemical processes that control how soil pH
668 affects phosphorus availability to plants. *Agriculture* 9, 120.

669 Price, H.L., Teasdale, P.R., Jolley, D.F., 2013. An evaluation of ferrihydrite- and Metsorb™-DGT techniques
670 for measuring oxyanion species (As, Se, V, P): Effective capacity, competition and diffusion coefficients.
671 *Analytica Chimica Acta* 803, 56-65.

672 Randall, G., Hoef, R., 1988. Placement methods for improved efficiency of P and K fertilizers: A review.
673 *Journal of Production Agriculture* 1, 70-79.

674 Robertson, D., Teasdale, P.R., Welsh, D.T., 2008. A novel gel - based technique for the high resolution,
675 two - dimensional determination of iron (II) and sulfide in sediment. *Limnology and Oceanography:
676 methods* 6, 502-512.

677 Santner, J., Prohaska, T., Luo, J., Zhang, H., 2010. Ferrihydrite containing gel for chemical imaging of labile
678 phosphate species in sediments and soils using diffusive gradients in thin films. *Analytical chemistry* 82,
679 7668-7674.

680 Santner, J., Zhang, H., Leitner, D., Schnepf, A., Prohaska, T., Puschenreiter, M., Wenzel, W.W., 2012. High-
681 resolution chemical imaging of labile phosphorus in the rhizosphere of *Brassica napus* L. cultivars.
682 *Environmental and Experimental Botany* 77, 219-226.

683 Shiva, A.H., Teasdale, P.R., Bennett, W.W., Welsh, D.T., 2015. A systematic determination of diffusion
684 coefficients of trace elements in open and restricted diffusive layers used by the diffusive gradients in a
685 thin film technique. *Analytica chimica acta* 888, 146-154.

686 Sissingh, H., 1983. Estimation of plant-available phosphates in tropical soils. A new analytical technique.
687 Haren, Netherlands, Inst Soil Fertility Research.

688 Syers, J., Johnston, A., Curtin, D., 2008. Efficiency of soil and fertilizer phosphorus use. *FAO Fertilizer and
689 plant nutrition bulletin* 18.

690 Teasdale, P.R., Hayward, S., Davison, W., 1999. In situ, high-resolution measurement of dissolved sulfide
691 using diffusive gradients in thin films with computer-imaging densitometry. *Analytical chemistry* 71, 2186-
692 2191.

693 White, S., Cordell, D., Moore, D., 2010. Securing a sustainable phosphorus future for Australia:
694 implications of global phosphorus scarcity and possible solutions.

695 Zhang, H., Davison, W., 1994. In situ speciation measurements of trace components in natural-waters
696 using thin-film gels. *Nature* 367, 546–548.

697 Zhang, H., Davison, W., 1995. Performance Characteristics of Diffusion Gradients in Thin Films for the In
698 Situ Measurement of Trace Metals in Aqueous Solution. *Anal. Chem.* 69, 3391-3400.

699 Zhang, H., Davison, W., Gadi, R., Kobayashi, T., 1998. In situ measurement of dissolved phosphorus in
700 natural waters using DGT. *Analytica Chimica Acta* 370, 29-38.

701 Zhu, Y., Shan, B., Huang, J., Teasdale, P.R., Tang, W., 2019. In situ biochar capping is feasible to control
702 ammonia nitrogen release from sediments evaluated by DGT. *Chemical Engineering Journal* 374, 811-821.

703

704